



Human Family With Sequence Similarity 83 Member B (FAM83B)



A Target Enabling Package (TEP)

| | |
|---------------------------------------|--|
| Gene ID / UniProt ID / EC | 222584 / Q5T0W9 / - |
| Target Nominator | Gopal Sapkota (University of Dundee) |
| SGC Authors | Daniel M. Pinkas, Joshua C. Bufton, Alice E. Fox, Gian Filippo Ruda, Romain Talon, Tobias Krojer, Anthony R. Bradley, Frank von Delft, Paul E. Brennan, Alex N. Bullock |
| Collaborating Authors | Luke J. Fulcher ¹ , Polyxeni Bozatz ¹ , Theresa Tachie-Menson ¹ , Kevin Z. L. Wu ¹ , Timothy D. Cummins ¹ , Karen Dunbar ¹ , Sabin Shrestha ¹ , Nicola T. Wood ¹ , Simone Weidlich ¹ , Thomas J. Macartney ¹ , Joby Varghese ¹ , Robert Gourlay ¹ , David G. Campbell ¹ , Fay Cooper ² , Luke D Hutchinson ¹ , Janis Vogt ¹ , Kevin S. Dingwell ² , James C. Smith ² , Gopal P. Sapkota ¹ |
| Target PI | Alex N. Bullock (SGC Oxford) |
| Therapeutic Area(s) | Cancer |
| Disease Relevance | Amplification or overexpression of FAM83B drives malignant transformation, poor prognosis and drug resistance in multiple cancers, including breast cancer. |
| Date Approved by TEP Evaluation Group | 13 th June 2018 |
| Document version | 1 |
| Document version date | May 2018 |
| Citation | Daniel M. Pinkas, Joshua C. Bufton, Alice E. Fox, Gian Filippo Ruda, Romain Talon, Tobias Krojer, ... Alex N. Bullock. (2018). Human Family With Sequence Similarity 83 Member B (FAM83B); A Target Enabling Package. Zenodo. http://doi.org/10.5281/zenodo.1342540 |
| Affiliations | ¹ MRC Protein Phosphorylation and Ubiquitylation Unit, University of Dundee ² The Francis Crick Institute, London |

We respectfully request that this document is cited using the DOI reference as given above if the content is used in your work.

USEFUL LINKS



Open Targets



(Please note that the inclusion of links to external sites should not be taken as an endorsement of that site by the SGC in any way)

SUMMARY OF PROJECT

FAM83A-H are newly identified oncogenes characterised by a conserved DUF1669 domain. FAM83B can substitute for RAS to promote malignant transformation. Ablation of FAM83B or mutation of Lys230 inhibits malignant phenotypes, implicating FAM83B as potential therapeutic target. As part of this TEP, we solved the first crystal structures from the FAM83 family, including FAM83A and FAM83B. The structures of the DUF1669 domain reveal a phospholipase D-like fold lacking conservation of key catalytic residues. We deorphanise the FAM83 DUF1669 domain as a critical docking scaffold for binding of casein kinase 1 isoforms. Finally, using XChem fragment screening we report chemical fragments that bind to Lys230 in the central pocket of the DUF1669 and form starting points for potential drug development.

SCIENTIFIC BACKGROUND

The FAM83 (family with sequence similarity 83) protein family includes eight members (FAM83A-H) that contain a Domain of Unknown Function 1669 (DUF1669) at their N-terminus and a variable C-terminus (**Fig. 1A**) (1,2).

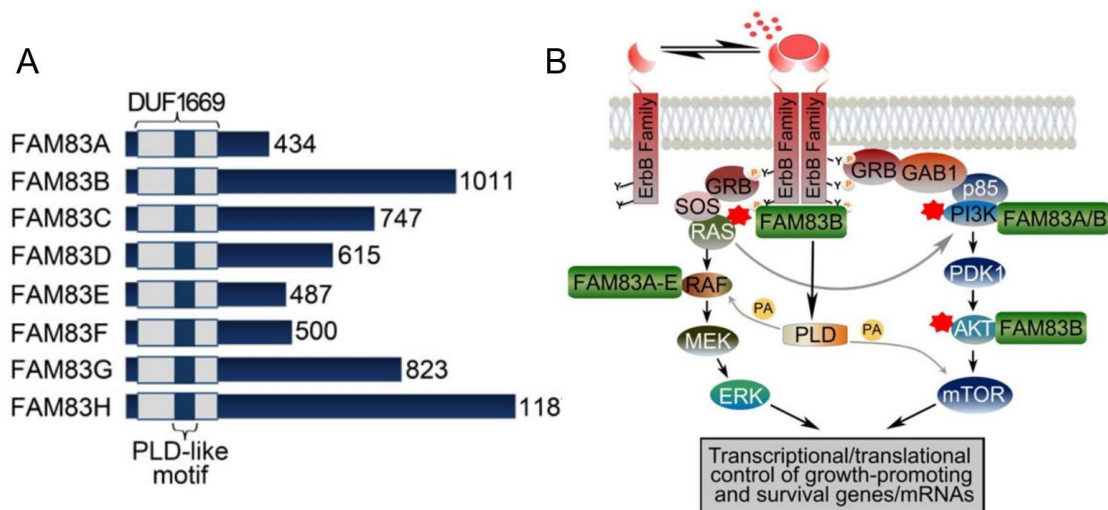


Fig. 1. FAM83 family proteins and signalling. **(A)** FAM83 proteins share a conserved DUF1669 domain at their N-terminus. **(B)** Schematic for FAM83 protein involvement in oncogenic signalling pathways. Figure adapted from (1).

FAM83 members show increased DNA copy number and /or overexpression in many tumour types and are associated with poor prognosis and drug resistance in a broad range of cancers (2,3). Here we focus on FAM83A and FAM83B. FAM83A was first reported in lung cancers as the tumour specific antigen BJ-TSA-9 (4). FAM83A amplification was also found in pancreatic cancer where it was reported to promote cancer stem cell-like traits and chemoresistance (5). Elevated FAM83A levels were similarly detected in breast cancers and knockdown suppressed the growth of breast cancer cells in both 2D and 3D cultures (1) and delayed tumour growth in mice (6). Genetic screens identified FAM83B as a gene that could substitute for RAS to transform human mammary epithelial cells (HMECs) (7). FAM83B overexpression was so far observed in breast, bladder, testis, ovary, thyroid, pancreatic and lung cancers (1-3). FAM83B protein associated in cells with common oncogenic signalling pathways including the EGFR, PI3K-mTOR, RAF and MAPK pathways and caused drug resistance to targeted therapies (**Fig. 1B**) (1,2,8). Knockdown of FAM83B inhibited proliferation of breast and lung cancer cells as well as tumorigenicity in vivo (7,9). Together, these data strongly implicate FAM83 proteins as potential therapeutic targets.

The DUF1669 domain has a predicted phospholipase D fold. However, the catalytic motif, HxK(xxxx)D(xxxxx)GSxN, is conserved only in FAM83D and no phospholipase activity has been detected for FAM83B (8). Interestingly, elevated FAM83B expression was associated with increased activity of canonical Phospholipase D enzymes and the growth of breast epithelial HME1 cells was inhibited by both FAM83B knockdown and by PLD1 small molecule inhibitors (8). The DUF1669 of FAM83B was necessary and sufficient to drive HME1 transformation. Moreover, site-directed mutagenesis of Lys230 (corresponding to the pseudoactive site HxK position) prevented FAM83B-EGFR association and suppressed FAM83B-mediated oncogenic signalling and anchorage-independent growth (8). Thus, the DUF1669 domain and pseudoactive site in particular are identified as relevant sites for drug targeting.

As part of this TEP, we characterise the structure and function of the DUF1669 domain and establish initial chemical starting points for inhibitor development.

RESULTS – THE TEP

Proteins purified

FAM83A DUF1669 domain (used for crystallography, assays)

Human FAM83A DUF1669 domain (a.a. 122-304) was cloned into pNIC28-Bsa4, expressed in BL21(DE3)-R3-pRARE2 cells and purified sequentially using Ni-affinity, cation exchange and size exclusion chromatography.

FAM83B DUF1669 domain (used for crystallography, assays)

Human FAM83B DUF1669 domain (a.a. 117-294) was cloned into pNIC28-Bsa4, expressed in BL21(DE3)-R3-pRARE2 cells and purified sequentially using Ni-affinity and size exclusion chromatography.

FAM83A DUF1669 domain biotinylated (used for assays)

Human FAM83A DUF1669 domain (a.a. 122-304) was cloned into pNIC-Bio3, expressed in BL21(DE3)-R3-pRARE2-BirA cells and purified sequentially using Ni-affinity and size exclusion chromatography. Biotinylated protein was prepared in vivo by inoculation of cultures with a solution of biotin and bicine.

FAM83B DUF1669 domain biotinylated (used for assays)

Human FAM83B DUF1669 domain (a.a. 117-294) was cloned into pNIC-Bio3, expressed in BL21(DE3)-R3-pRARE2-BirA cells and purified sequentially using Ni-affinity and size exclusion chromatography. Biotinylated protein was prepared in vivo by inoculation of cultures with a solution of biotin and bicine.

CSNK1D (used for assays)

Human CSNK1D (a.a. 1-294) was cloned into pNIC28-Bsa4, expressed in BL21(DE3)-R3-pRARE2 cells and purified sequentially using Ni-affinity and size exclusion chromatography.

CSNK1E (used for assays)

Human CSNK1E (a.a. 1-294) was cloned into pNIC28-Bsa4, expressed in BL21(DE3)-R3-pRARE2 cells and purified sequentially using Ni-affinity and size exclusion chromatography.

Structural data

Novel FAM83 family structures

4URJ 2.68 Å structure of FAM83A DUF1669 domain
5LZK 1.58 Å structure of FAM83B DUF1669 domain

FAM83B fragment screening structures

5QHI 1.78 Å structure of FAM83B with fragment FM001923a
5QHJ 1.76 Å structure of FAM83B with fragment FM002203a
5QHK 1.72 Å structure of FAM83B with fragment FM001730a
5QHL 1.80 Å structure of FAM83B with fragment FM001894a
5QHM 1.84 Å structure of FAM83B with fragment FM000368b
5QHN 1.81 Å structure of FAM83B with fragment FM002168a
5QHO 1.74 Å structure of FAM83B with fragment FM001730a
5QHP 2.10 Å structure of FAM83B with fragment XS094794b
5QHQ 2.03 Å structure of FAM83B with fragment FM001992a
5QHR 1.95 Å structure of FAM83B with fragment FM002208b
5QHS 1.95 Å structure of FAM83B with fragment FF000014a

Novel structural features of the FAM83 DUF1669 domain

The novel DUF1669 domain structures of FAM83A and FAM83B show the predicted phospholipase D (PLD) fold (**Fig. 2**). The first structure solved with this fold was the bacterial endonuclease Nuc (PDB [1BYR](#)) (10), which shares 19.7% sequence identity with FAM83A. Overall, the FAM83 and bacterial Nuc proteins form a

conserved dimeric structure about a two-fold axis. The monomers share a central eight-stranded β -sheet flanked on one side by helices $\alpha 1$, $\alpha 2$, $\alpha 3$ and on the other side by $\alpha 5$; a smaller helix $\alpha 4$ is positioned in the plane of the sheet. Differences between the FAM83 fold and other PLD family members are evident in two structural regions. First, the FAM83 fold contains a large β -hairpin insertion between the usual $\beta 4$ and $\beta 5$ strands (**Fig. 2**). Second, the $\alpha 3$ helix in FAM83A and FAM83B is oriented approximately perpendicularly to the equivalent helix in Nuc (**Fig. 2**). Interestingly, both structural elements in the FAM83 fold help to frame the central pocket which is the catalytic site in other active PLD family enzymes.

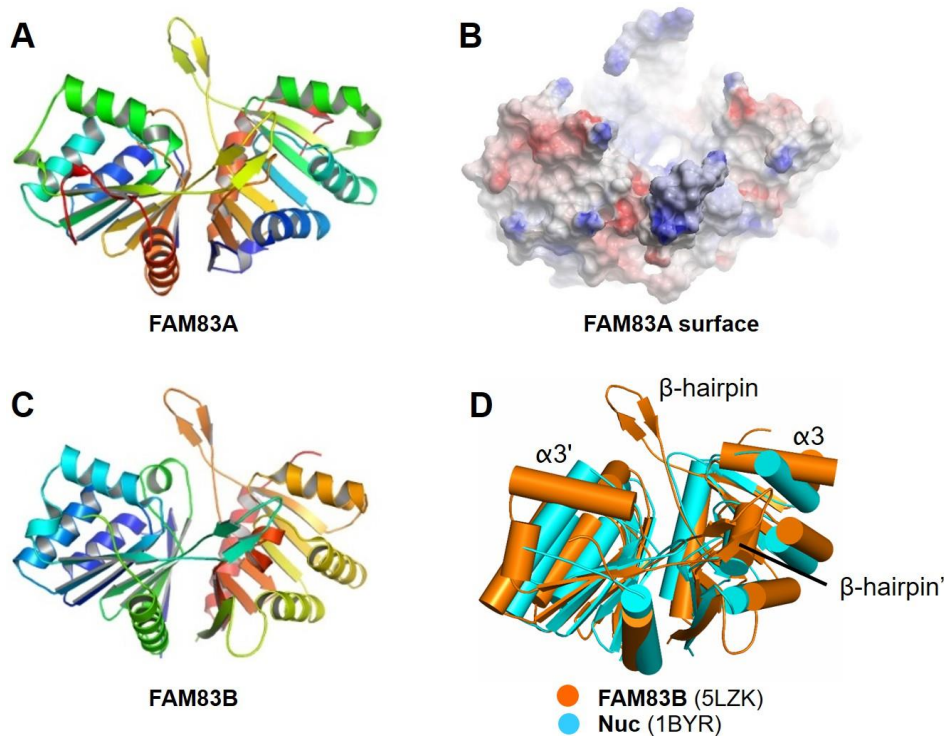


Fig. 2. First FAM83-family structures. **(A)** FAM83A dimer. **(B)** FAM83A molecular surface coloured by electrostatic surface potential highlighting the central pocket. **(C)** FAM83B dimer. **(D)** Superposition of FAM83B and the bacterial endonuclease Nuc. The FAM83-specific β -hairpin and rotated $\alpha 3$ helix are labelled in each monomer.

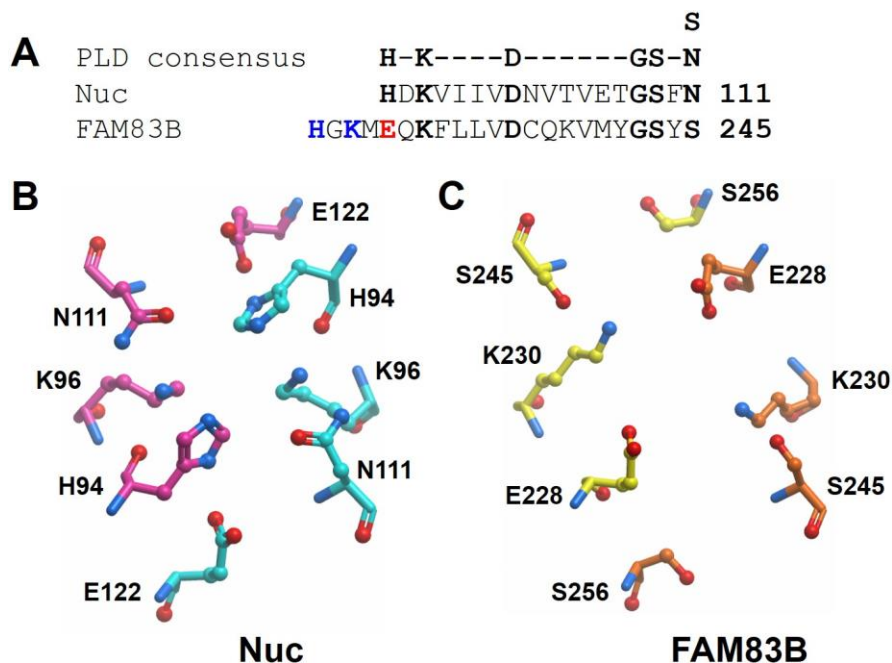


Fig. 3. Active site comparisons. **(A)** Sequence alignment of the PLD consensus motif in Nuc and FAM83 proteins. **(B)** Packing of selected active site residues in **(B)** Nuc dimer and **(C)** FAM83B dimer.

The Lys230 residue in FAM83B (critical for oncogenic effects) is structurally conserved with the catalytic HxK motif in Nuc (**Fig. 3**), but the histidine is replaced in FAM83B by a glutamate. Interestingly, an alternative HxK motif is positioned just upstream in FAM83B provided by the FAM83-specific β -hairpin (**Fig. 3**). However, these residues would not be proximal to the other suggested catalytic residues and may alternatively form a part of a novel binding site.

Further structural features relating to inhibitor design are described later in this document.

Assays of FAM83 Function

FAM83 proteins bind to casein kinase I isoforms

To uncover potential roles of the FAM83 family and the DUF1669 domain, our collaborators undertook a comprehensive proteomic study in HEK293 cells using mass spectrometry. Significantly, this study revealed that all FAM83 members could interact with Casein Kinase 1 (CSNK1) α , α -like, δ , and ϵ isoforms, while γ isoform binding was not detected. The precise abundance of the recovered CSNK isoforms varied with each FAM83 member suggestive of certain levels of specificity. Detailed results and experimental procedures are published (11).

We investigated these interactions further using purified recombinant proteins for the CSNK1 kinase domain and FAM83 DUF1669 domain. A first assay using a pull down approach revealed a direct interaction between the two proteins that appears independent of post-translational modifications (**Fig. 4A**). Binding affinity measurements using biolayer interferometry on an Octet RED384 instrument indicated a dissociation constant (K_D) of 5 μ M (**Fig. 4B**). Preliminary attempts to co-crystallise these complexes have so far been unsuccessful.

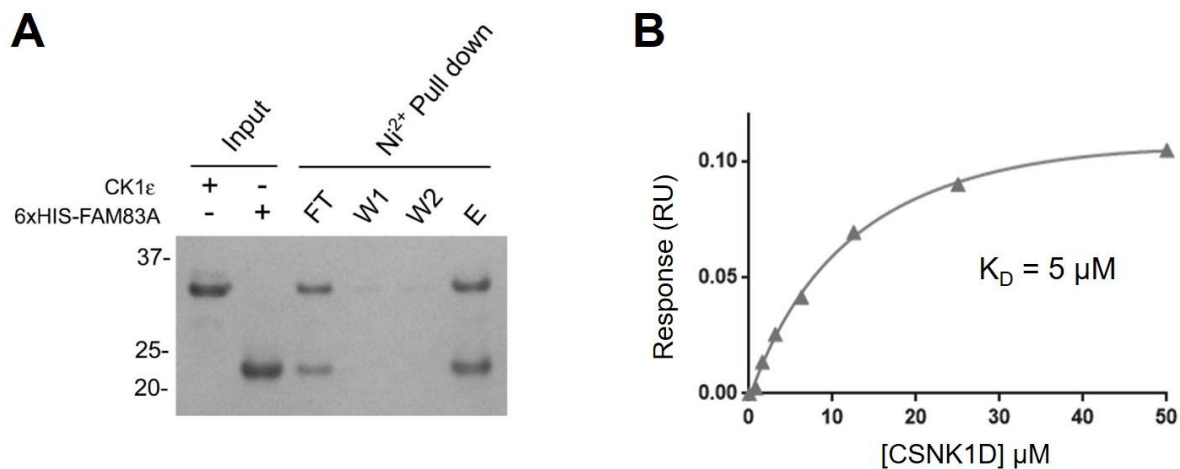


Fig. 4. FAM83 proteins bind to casein kinase 1 isoforms. **(A)** Pull down experiment showing direct binding of CSNK1E (CK1 ϵ) kinase domain and FAM83A DUF1669 domain. **(B)** Biolayer interferometry study showing binding of CSNK1D kinase domain to the FAM83B DUF1669 domain.

FAM83-Casein kinase 1 interactions are functionally important

Our collaborators used U2OS cells stably integrated with Tet-inducible expression of GFP-alone (negative control) or GFP-FAM83 members to explore their subcellular localisation by fluorescence microscopy, as well as that of CSNK1A (CK1 α) visualised by antibody staining. When co-expressed FAM83B and CSNK1A were co-localised with pan-cellular staining along with additional membrane punctate structures (**Fig. 5A**). This pattern was distinct to that observed in cells expressing either GFP or CSNK1A alone (**Fig. 5A**). Further results and details are published suggesting that FAM83 proteins might scaffold and anchor CSNK1 isoforms to organise their signal transduction in cells (11). Consequently, we propose that the DUF1669 be renamed the Polypeptide Anchor of CK1 (PACK1) domain.

CSNK1A controls developmental signal transduction cascades through phosphorylation of β -catenin in the absence of WNT. Our collaborators found a profound effect of FAM83G expression on WNT-specific phenotypes. Specifically, injection of mRNA for FAM83G (also known as PAWS1) into *Xenopus* embryos caused the activation of WNT signalling and axis duplication (**Fig. 5B**). These results suggested that the co-localisation of FAM83 and CSNK1 isoforms was functionally relevant and are recently published in *EMBO Reports* (12).

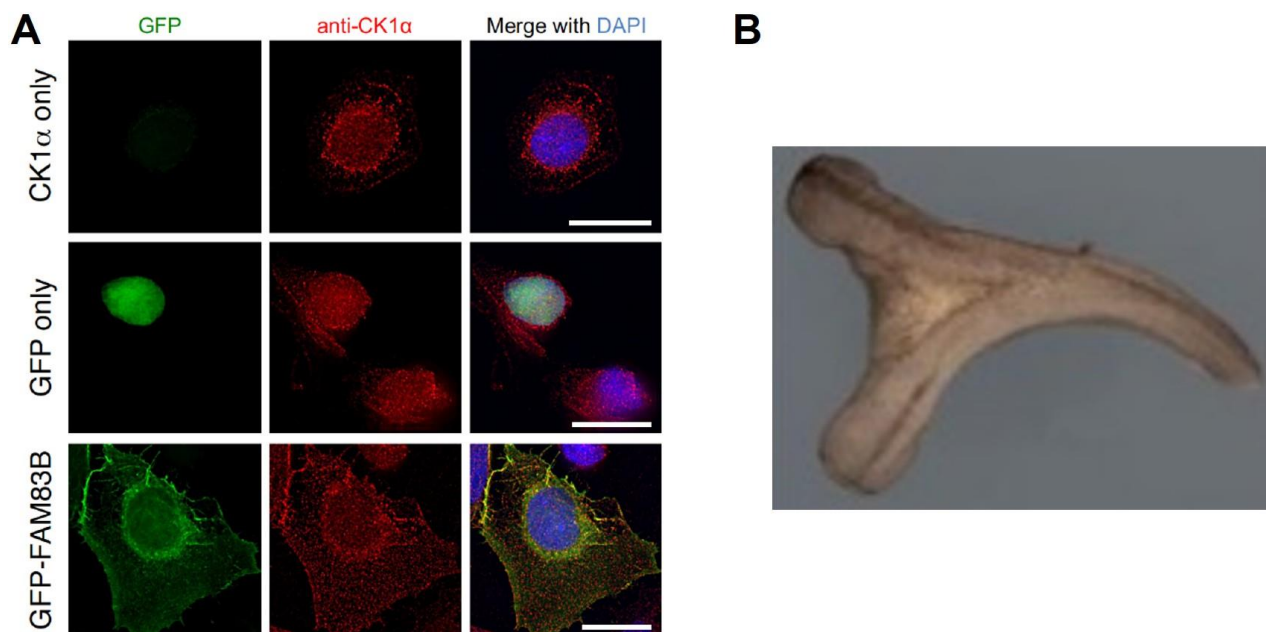


Fig. 5. Functional relevance of FAM83-CSNK1 interactions. **(A)** Co-localisation of FAM83B and CSNK1A (CK1 α) in U2OS cells stably integrated with Tet-inducible GFP-alone (negative control) or GFP-FAM83B. Representative images are shown (GFP-FAM83B (n=56); GFP only (n=38); CK1 α only (n=82)). Scale bars represent 20 μ m. **(B)** Injection of FAM83G mRNA into *xenopus* embryos causes axis duplication (published in (12)).

Assays of FAM83 binding to small molecule inhibitor fragments

XChem fragment screening

The XChem platform at the Diamond Light Source was used for crystallography-based fragment screening against the human FAM83B DUF1669 domain. FAM83B was chosen due to the high resolution of its solved crystal structure (1.6 Å) versus that of the equivalent FAM83A domain (2.7 Å). Midway through the screening of FAM83B it was apparent that the crystal packing in the known crystal form (P2₁) prevented access of fragments to the primary central pocket containing the critical residue Lys230. An alternative crystal form (P4₁22) suitable for soaking into this site was identified by further exploration of viable crystallisation conditions and was used for all subsequent XChem work.

In total over 800 fragments were screened covering compounds from the DSPL1, DSPL2 and OxXchem chemical libraries. Bound fragments were identified using PanDDA (13) in the context of the XChemExplorer software suite and their co-crystal structures refined using REFMAC (14). 9 fragment hits were identified during screening (**Fig. 6**), of which 1 fragment (FM000368b, also known as OX145) was bound specifically to the primary site of interest, Lys230 in the central pocket of the PLD fold (**Fig. 7**). Further exploration of this fragment scaffold is underway to establish its structure-activity relationship, but has already identified a similar binding mode for the fragment analogue FF000014a (**Fig. 6**).

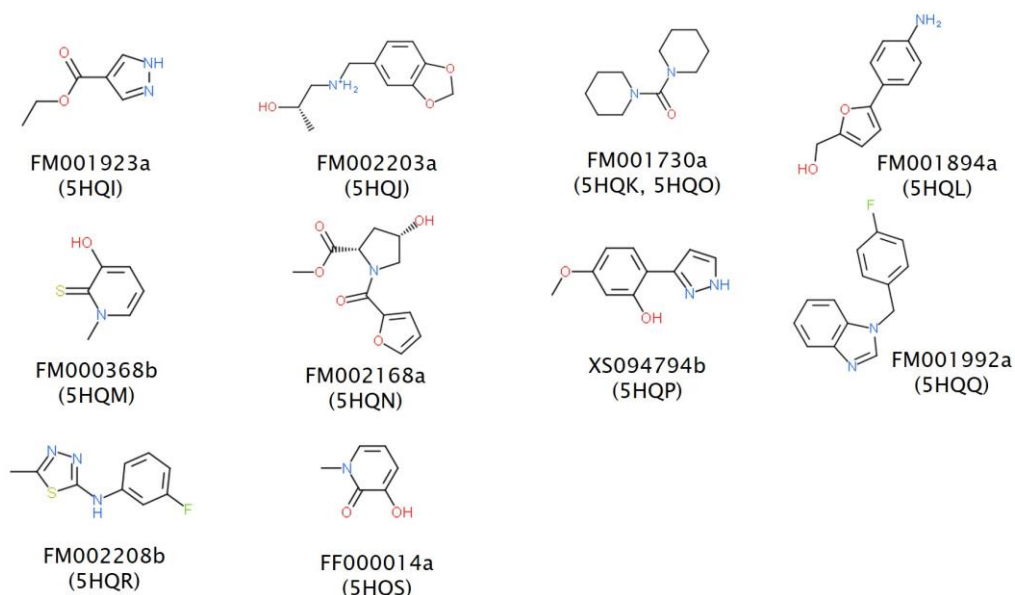


Fig. 6. XChem fragment screening hits. To date 10 binding fragments have been identified for FAM83B.

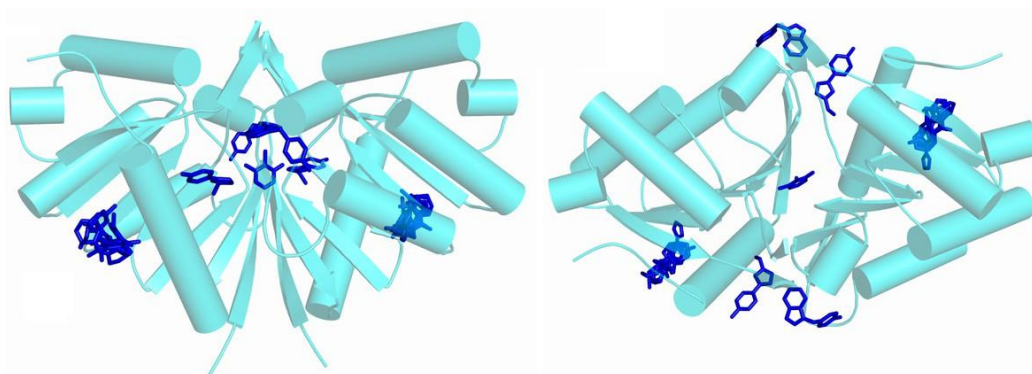


Fig. 7. XChem screening fragment binding sites. One fragment FM000368b, also known as OX145, was of specific interest due to its binding at the central pocket.

Fragment binding affinities

Selected fragments identified by XChem crystallography were analysed for their binding affinities by surface plasmon resonance (SPR) using a Biacore S200 instrument. For these experiments, we prepared biotinylated FAM83A and FAM83B proteins for immobilisation on streptavidin-coated sensor chips. Fragments FM000368b and FF000014a, which occupied the central pocket, bound to FAM83B with K_D values of $\sim 50 \mu\text{M}$ (**Fig. 8**) yielding ligand efficiencies >0.65 . Similar binding was observed to FAM83A suggesting potential to develop these fragments in parallel against other FAM83 family members (**Fig. 8**).

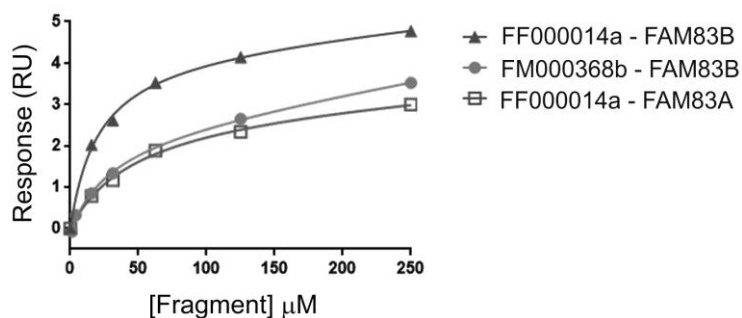


Fig. 8. SPR measurements. Fragment binding affinities were determined using a Biacore S200 instrument and yielded K_D values of $\sim 50 \mu\text{M}$.

Chemical Matter

Primary fragments of interest

Fragments FM000368b and FF000014a form the primary chemical matter in this TEP (**Fig. 9**).

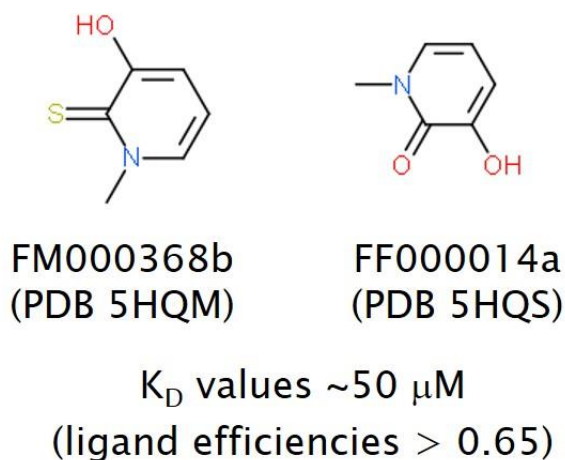


Fig. 9. Primary chemical matter. Fragments FM000368b and FF000014a were selected for further development based on their binding to the functionally relevant central pocket (work ongoing).

Pocket shape and fragment interactions

The FAM83B co-crystal structure with fragment FM000368b reveals binding at the base of the central pocket where the compound sits between the two symmetry-related Lys230 residues in the FAM83B dimer (**Fig. 10**).

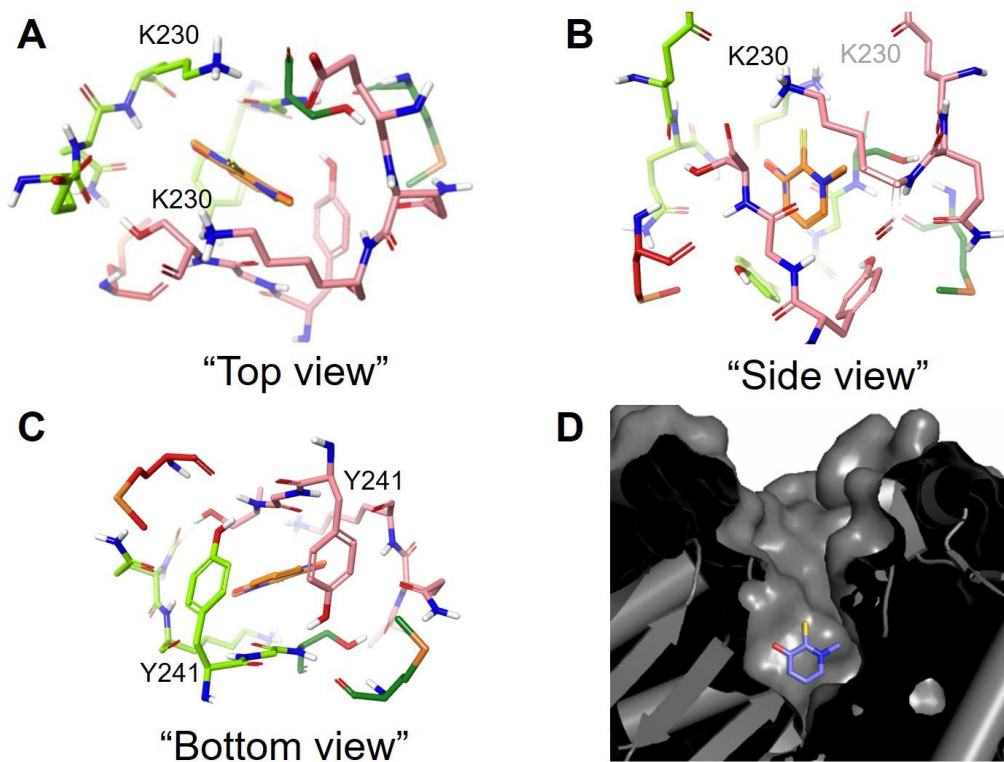


Fig. 10. Binding mode of the FM000368b fragment showing different views (A-D).

Follow up chemistry

Further screening and chemistry around the FM000368b fragment is ongoing, but has led to the identification of FF000014a, in which an oxygen replaces the sulphur atom (**Fig. 9**). Comparison of the co-crystal structures of these two fragments suggests a slight rotation of the aromatic ring that would alter the potential site preferences for derivatisation (**Fig. 11**).

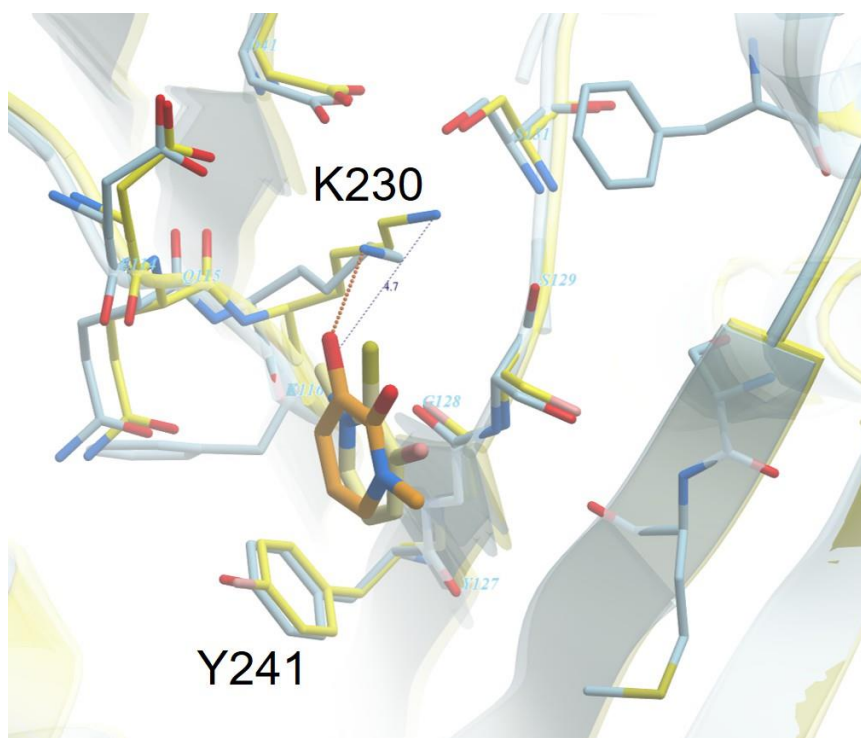
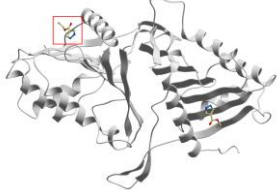
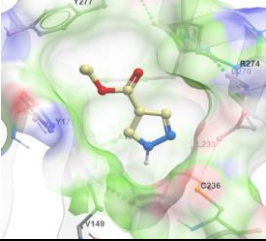
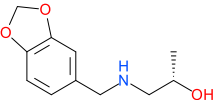
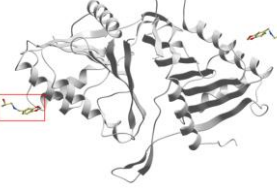
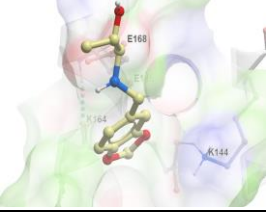
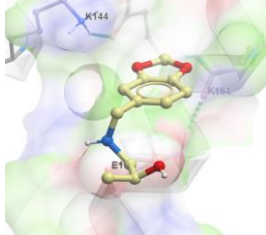
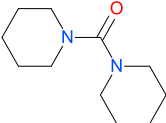
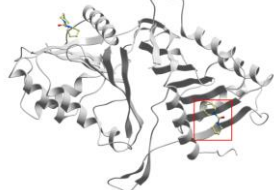
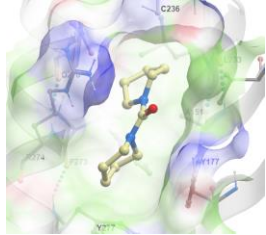
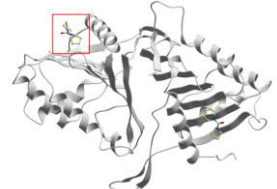
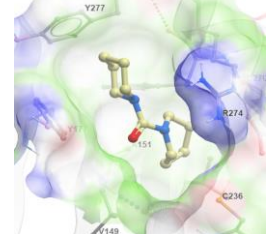
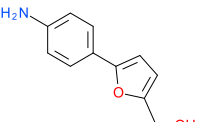
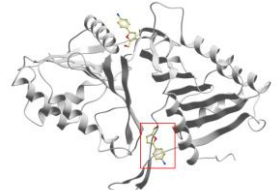
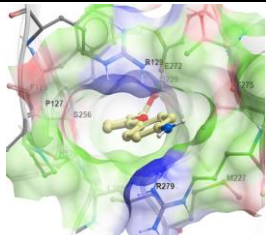
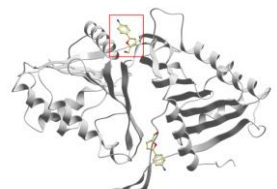
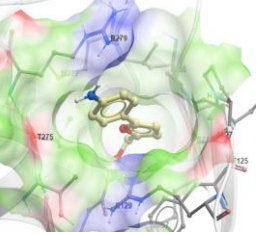
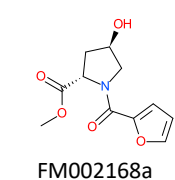
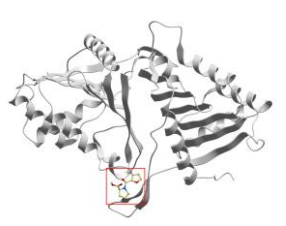
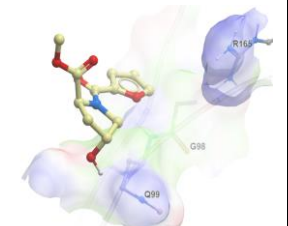
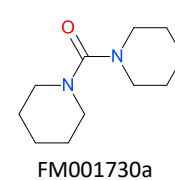
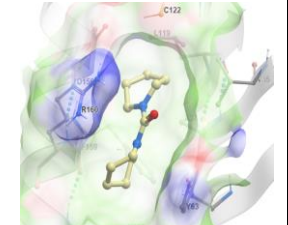
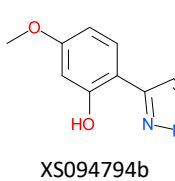
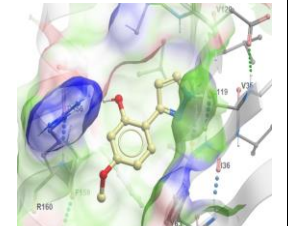
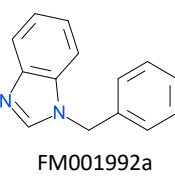
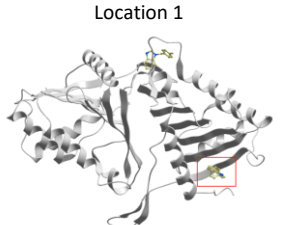
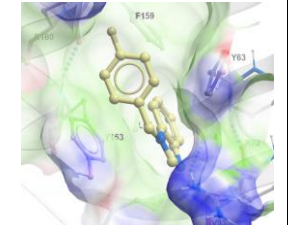
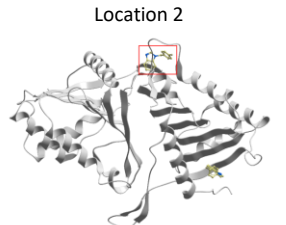
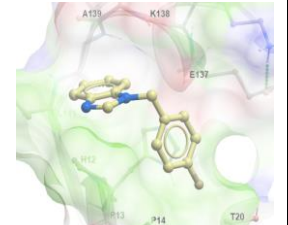
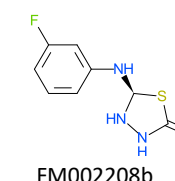
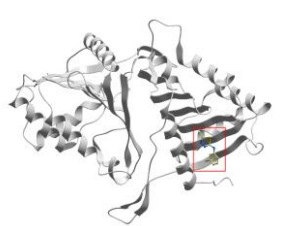
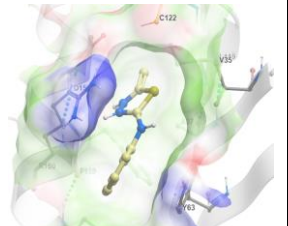


Fig. 11. Superposition of FAM83B structures bound to fragments FM000368b and FF000014a, respectively.

Overview of FAM83B and bound fragments

| PDBID | Ligand | Binding Location | Binding pocket | Resolution (Å) |
|-------|---------------|------------------|----------------|----------------|
| 5QHM | FM000368b | | | 1.84 |
| 5QHS | FF000014a | | | 1.95 |
| 5QHI | FM001923a | Location 1 | | 1.78 |

| | | | | |
|------|--|---|--|------|
| | | Location 2  |  | |
| 5QHJ |  FM002203a | Location 1  |  | 1.76 |
| | | Location 2  |  | |
| 5QHK |  FM001730a | Location 1  |  | 1.72 |
| | | Location 2  |  | |
| 5QHL |  FM001894a | Location 1  |  | 1.80 |
| | | Location 2  |  | |

| | | | | |
|------|--|---|--|------|
| 5QHN |  FM002168a |  |  | 1.81 |
| 5QHO |  FM001730a |  |  | 1.74 |
| 5QHP |  XS094794b |  |  | 2.10 |
| 5QHQ |  FM001992a | Location 1  |  | 2.03 |
| | | Location 2  |  | |
| 5QHR |  FM002208b |  |  | 1.95 |

IMPORTANT: Please note that the existence of small molecules within this TEP only indicates that chemical matter can bind to the protein in a functionally relevant pocket. As such, these molecules should not be used as tools for functional studies of the protein unless otherwise stated as they are not sufficiently potent or well-characterised to be used in cellular studies. The small molecule ligands are intended to be used as the basis for future chemistry optimisation to increase potency and selectivity and yield a chemical probe or lead series.

Antibodies

Commercial antibodies against FAM83A and FAM83B are available and validated in the literature, although they have not been tested at the SGC.

CRISPR/Cas9 reagents

Our collaborator Gopal Sapkota (MRC PPU, Dundee) has validated CRISPR/Cas9 reagents for knock-out of FAM83A and FAM83B as well as knock-ins of their GFP fusions (published in (11)).

Future plans

Further chemistry for development of fragments FM000368b and FF000014a is ongoing supported by a MRC confidence in concept award. Additional characterisation of FAM83 interactions with casein kinase 1 isoforms is also in progress with the aim ultimately to determine their co-crystal structure. We are also preparing ScFv fragments against these proteins using phage display.

Collaborations

Proteomics: Gopal Sapkota (University of Dundee)
Xenopus assays: Jim Smith (Francis Crick Institute)
ScFv selections: Susanne Grasland (SGC Stockholm)

CONCLUSION

FAM83 family proteins are a newly identified oncogenes that can promote tumour growth, poor prognosis and drug resistance in a variety of human cancers. Here we revealed that the N-terminal DUF1669 domain of these proteins forms a dimeric structure with a phospholipase D-like fold. While the catalytic histidine of the PLD HxK motif appears absent in FAM83B, the lysine (K230) is known to be critical to support oncogenic signalling and tumour growth (8). We showed that the DUF1669 domain forms a direct interaction with casein kinase 1 isoforms that appears to determine their co-localisation and thereby control their cellular function. This is significant as casein kinase 1 isoforms are already implicated in tumorigenesis (15).

We also utilized the XChem fragment screening technology to identify chemical starting points for drug development against FAM83B. Importantly, fragments bound in the main central pocket formed direct interaction with Lys230. Moreover, they exhibited significant binding affinity and ligand efficiency. The fragments, structures, assays and biotinylated proteins in this TEP form a valuable toolkit to explore FAM83 biology in future and to develop the first FAM83B inhibitors.

FUNDING INFORMATION

The work performed at the SGC has been funded by a grant from the Wellcome [106169/ZZ14/Z]. Follow up work for fragment screening by XChem was supported by a MRC Confidence in Concept Award.

ADDITIONAL INFORMATION

Structure Files

| PDB ID | Structure Details | Supplier |
|----------------------|--|-------------------|
| 4URJ | 2.68 Å structure of FAM83A DUF1669 domain | |
| 5LZK | 1.58 Å structure of FAM83B DUF1669 domain | |
| 5QHI | 1.78 Å structure of FAM83B with fragment FM001923a | Apollo Scientific |
| 5QHJ | 1.76 Å structure of FAM83B with fragment FM002203a | Specs |
| 5QHK | 1.72 Å structure of FAM83B with fragment FM001730a | Alfa Aesar |
| 5QHL | 1.80 Å structure of FAM83B with fragment FM001894a | IBScreen |
| 5QHM | 1.84 Å structure of FAM83B with fragment FM000368b | OxXChem |
| 5QHN | 1.81 Å structure of FAM83B with fragment FM002168a | Key Organics |
| 5QHO | 1.74 Å structure of FAM83B with fragment FM001730a | Alfa Aesar |
| 5QHP | 2.10 Å structure of FAM83B with fragment XS094794b | IBScreen |
| 5QHQ | 2.03 Å structure of FAM83B with fragment FM001992a | IBScreen |
| 5QHR | 1.95 Å structure of FAM83B with fragment FM002208b | Maybridge |
| 5QHS | 1.95 Å structure of FAM83B with fragment FF000014a | Gian Filippo Ruda |

Materials and Methods

Mass Spectrometry

Protein masses were determined using an Agilent LC/MSD TOF system with reversed-phase high-performance liquid chromatography coupled to electrospray ionization and an orthogonal time-of-flight mass analyser. Proteins were desalted prior to mass spectrometry by rapid elution off a C3 column with a gradient of 5-95% isopropanol in water with 0.1% formic acid. Spectra were analysed using the MassHunter software (Agilent).

Protein Expression and Purification

Human FAM83A DUF1669 domain

Boundaries: residues 122-304

Vector: pNIC28-Bsa4

Tag and additions: TEV-cleavable N-terminal hexahistidine tag

Expression cell: E. coli BL21(DE3)R3-pRARE2

FAM83A was expressed from the vector pNIC28-Bsa4 in BL21(DE3)-R3-pRARE cells (a phage-resistant derivative of Rosetta2, Novagen). Cultures (1 litre) in LB medium supplemented with 50 µg/mL kanamycin and 34 µg/mL chloramphenicol were incubated at 37°C until OD600 reached 0.8 and then cooled to 18°C and supplemented with 0.4 mM isopropyl 1-thio-β-D-galactopyranoside (IPTG) to induce protein expression overnight. Cells were harvested by centrifugation at 5000g, resuspended in binding buffer (50 mM HEPES pH 7.5, 500 mM NaCl, 5 mM imidazole, 5% glycerol) with 0.5 mM TCEP and EDTA-free complete protease inhibitor cocktail (Merck) and flash frozen. On thawing, the resuspended cell pellets were lysed by sonication. Lysates were clarified by centrifugation in a JA 25.50 rotor at 21500 rpm. The His6-tagged protein was immobilised on Ni²⁺-Sephacrose resin and bound proteins eluted using stepwise gradients of 50-250 mM imidazole in binding buffer. Removal of the His6 tag was performed at 4°C overnight using TEV protease. FAM83A was further purified by size exclusion chromatography using a Superdex 200 16/60 column (GE Healthcare) equilibrated in buffer containing 50mM HEPES pH 7.5, 300mM NaCl and 0.5mM TCEP. FAM83A was concentrated using centrifugal ultrafiltration with a 10 kDa molecular weight cut-off point membrane. Purity was confirmed by SDS-PAGE and identity verified by intact mass spectrometry.

Human FAM83B DUF1669 domain

Boundaries: residues 117-294

Vector: pNIC28-Bsa4

Tag and additions: TEV-cleavable N-terminal hexahistidine tag

Expression cell: E. coli BL21(DE3)R3-pRARE2

FAM83B was expressed from the vector pNIC28-Bsa4 in BL21(DE3)-R3-pRARE cells (a phage-resistant derivative of Rosetta2, Novagen). Cultures (1 litre) in LB medium supplemented with 50 µg/mL kanamycin and 34 µg/mL chloramphenicol were incubated at 37°C until OD600 reached 0.6 and then cooled to 18°C and supplemented with 0.35 mM isopropyl 1-thio-β-D-galactopyranoside (IPTG) to induce protein expression overnight. Cells were harvested by centrifugation at 5000g, resuspended in binding buffer (50 mM HEPES pH 7.5, 500 mM NaCl, 5 mM imidazole, 5% glycerol) with 0.5 mM TCEP and EDTA-free complete protease inhibitor cocktail (Merck) and flash frozen. On thawing, the resuspended cell pellets were lysed by sonication. Lysates were clarified by centrifugation in a JA 25.50 rotor at 21000 rpm. The His6-tagged protein was immobilised on Ni²⁺-Sephacrose resin and bound proteins eluted using stepwise gradients of 50-250 mM imidazole in binding buffer. Removal of the His6 tag was performed at 4°C overnight using TEV protease. FAM83B was further purified by size exclusion chromatography using a Superdex 200 16/60 column (GE Healthcare) equilibrated in buffer containing 50 mM HEPES pH 7.5, 300 mM NaCl and 0.5 mM TCEP, followed by cation exchange chromatography. FAM83B was loaded onto a HiTrap S 5ml column in a buffer of 50 mM NaCl, 50 mM HEPES pH 7.5 and 0.5 mM TCEP and then eluted using a gradient of 1 M NaCl, 50 mM HEPES pH 7.5 and 0.5 mM TCEP. FAM83B was concentrated using centrifugal ultrafiltration with a 10 kDa molecular weight cut-off point membrane and diluted to a final salt concentration of 220 mM NaCl. Purity was confirmed by SDS-PAGE and identity verified by intact mass spectrometry.

Human FAM83A DUF1669 domain (biotinylated)

Boundaries: residues 122-304

Vector: pNIC-Bio3

Tag and additions: C-terminal biotinylation sequence and TEV-cleavable N-terminal hexahistidine tag

Expression cell: E. coli BL21(DE3)-R3-pRARE2-BirA

FAM83A was expressed from the vector pNIC-Bio3 in BL21(DE3)-R3-pRARE2-BirA cells. Cultures (1 litre) in LB medium supplemented with 50 µg/mL kanamycin, 34 µg/mL chloramphenicol and 50 µg/mL streptomycin were incubated at 37°C until OD600 reached 0.6 and then cooled to 18°C and supplemented with 0.4 mM IPTG and 100 µM biotin solution to induce biotinylated protein expression overnight. In the morning cultures were supplemented with a further 100 µM biotin solution and incubated for an hour before harvesting. Cells were harvested by centrifugation at 5000g, resuspended in binding buffer (50 mM HEPES pH 7.5, 500 mM NaCl, 5 mM imidazole, 5% glycerol, 0.5mM TCEP) with EDTA-free complete protease inhibitor cocktail (Merck) and flash frozen. On thawing, the resuspended cell pellets were lysed by sonication. Lysates were clarified by centrifugation in a JA 25.50 rotor at 21500 rpm. The His6-tagged protein was immobilised on Ni²⁺-Sephacrose resin and bound proteins eluted using stepwise gradients of 50-250 mM imidazole in binding buffer. Removal of the His6 tag was performed at 4°C overnight using TEV protease. FAM83A was further purified by size exclusion chromatography using a Superdex 200 16/60 column (GE Healthcare) equilibrated in buffer containing 50 mM HEPES pH 7.5, 300 mM NaCl and 0.5 mM TCEP. FAM83A was concentrated using centrifugal ultrafiltration with a 3 kDa molecular weight cut-off point membrane. Purity was confirmed by SDS-PAGE and identify and biotinylation verified by intact mass spectrometry.

Human FAM83B DUF1669 domain (biotinylated)

Boundaries: residues 117-294

Vector: pNIC-Bio3

Tag and additions: C-terminal biotinylation sequence and TEV-cleavable N-terminal hexahistidine tag

Expression cell: E. coli BL21(DE3)-R3-pRARE2-BirA

FAM83B was expressed from the vector pNIC-Bio3 in BL21(DE3)-R3-pRARE2-BirA cells. Cultures (1 litre) in LB medium supplemented with 50 µg/mL kanamycin, 34 µg/mL chloramphenicol and 50 µg/mL streptomycin were incubated at 37°C until OD600 reached 0.6 and then cooled to 18°C and supplemented with 0.4 mM IPTG and 100 µM biotin solution to induce biotinylated protein expression overnight. In the morning cultures were supplemented with a further 100 µM biotin solution and incubated for an hour before harvesting. Cells were harvested by centrifugation at 5000g, resuspended in binding buffer (50 mM HEPES pH 7.5, 500 mM NaCl, 5 mM imidazole, 5% glycerol, 0.5 mM TCEP) with EDTA-free complete protease inhibitor cocktail (Merck) and flash frozen. On thawing, the resuspended cell pellets were lysed by sonication. Lysates were clarified by centrifugation in a JA 25.50 rotor at 21500 rpm. The His6-tagged protein was immobilised on Ni²⁺-Sephacrose resin and bound proteins eluted using stepwise gradients of 50-250 mM imidazole in binding buffer. Removal of the His6 tag was performed at 4°C overnight using TEV protease. FAM83B was further purified by size exclusion chromatography using a Superdex 200 16/60 column (GE Healthcare) equilibrated in buffer containing 50 mM HEPES pH 7.5, 300 mM NaCl and 0.5 mM TCEP. FAM83B was concentrated using centrifugal ultrafiltration with a 3 kDa molecular weight cut-off point membrane. Purity was confirmed by SDS-PAGE and identify and biotinylation verified by intact mass spectrometry.

Human CSNK1D

Boundaries: residues 1-294

Vector: pNIC28-Bsa4

Tag and additions: TEV-cleavable N-terminal hexahistidine tag

Expression cell: E. coli BL21(DE3)R3-pRARE2

CSNK1D was expressed from the vector pNIC28-Bsa4 in BL21(DE3)-R3-pRARE cells (a phage-resistant derivative of Rosetta2, Novagen). Cultures (1 litre) in LB medium supplemented with 50 µg/mL kanamycin and 34 µg/mL chloramphenicol were incubated at 37°C until OD600 reached 0.6 and then cooled to 18°C and supplemented with 0.4 mM IPTG to induce protein expression overnight. Cells were harvested by centrifugation at 5000g, resuspended in binding buffer (50 mM HEPES pH 7.5, 500 mM NaCl, 5 mM imidazole, 5% glycerol, 0.5 mM TCEP) with EDTA-free complete protease inhibitor cocktail (Merck) and flash frozen. On

thawing, the resuspended cell pellets were lysed by sonication. Lysates were clarified by centrifugation in a JA 25.50 rotor at 21000 rpm. The His6-tagged protein was immobilised on Ni²⁺-Sepharose resin and bound proteins eluted using stepwise gradients of 50-250 mM imidazole in binding buffer. Removal of the His6 tag was performed at 4°C overnight using TEV protease. CSNK1D was further purified by size exclusion chromatography using a Superdex 200 16/60 column (GE Healthcare) equilibrated in buffer containing 50 mM HEPES pH 7.5, 300 mM NaCl and 0.5 mM TCEP before concentration using centrifugal ultrafiltration with a 10 kDa molecular weight cut-off point membrane. Purity was confirmed by SDS-PAGE and identity verified by intact mass spectrometry.

Human CSNK1E

Boundaries: residues 1-294

Vector: pNIC28-Bsa4

Tag and additions: TEV-cleavable N-terminal hexahistidine tag

Expression cell: E. coli BL21(DE3)R3-pRARE2

CSNK1E was expressed in E. coli strain BL21(DE3) R3-pRARE2 using the pNIC28-Bsa4 vector, which encodes for a N-terminal hexahistidine (6XHis) tag and TEV cleavage site. Cultures were grown at 37°C in LB medium supplemented with 50 µg/mL kanamycin and 34 µg/mL chloramphenicol to an OD of 0.6, before expression at 18°C overnight by induction with 0.4 mM isopropyl 1-thio-β-D-galactopyranoside. Cells were harvested by centrifugation at 5000 g and pellets resuspended in binding buffer (50 mM HEPES pH 7.5, 500 mM NaCl, 5% glycerol, 5 mM imidazole) supplemented with Calbiochem protease inhibitor set III. Cells were lysed by sonication before clarification of the lysate by centrifugation in a JA 25.50 rotor at 36,000 g. His-tagged proteins were immobilized on Ni-sepharose and bound proteins were eluted using step gradients of imidazole (50-250 mM). CSNK1E protein was cleaved with TEV protease overnight at 4°C and purified further by size exclusion chromatography using an S75 HiLoad 16/60 Superdex column equilibrated in buffer containing 50 mM HEPES pH 7.5, 300 mM NaCl, and 0.5 mM TCEP. Protein was concentrated by centrifugal ultrafiltration using a 3 kDa molecular weight cut-off concentrator. Protein concentration was determined by measuring absorbance at 280 nm. Protein purity of >95% was confirmed by SDS-PAGE and construct identity and tag cleavage were verified by mass spectrometry.

Structure Determination

FAM83A (PDB: 4URJ, 2.68 Å)

FAM83A DUF1669 domain (a.a 122-304) was buffered in 50 mM HEPES pH 7.5, 300 mM NaCl and concentrated to 12 mg/mL. Crystals were grown at 20°C in 150 nL sitting drops at a 1:2 protein: reservoir solution comprising 0.8 M sodium phosphate monobasic, 0.8 M potassium phosphate dibasic and 0.1 M HEPES pH 7.5. Before mounting, crystals were cryoprotected with mother liquor supplemented with an additional 25 % ethylene glycol and vitrified in liquid nitrogen. Diffraction data were collected at Diamond Light Source beamline I03. Diffraction data were processed using XDS (16) and molecular replacement was performed using PHENIX.MR_ROSETTA (17). Model building and refinement were done using COOT (18) and PHENIX (19).

FAM83B (PDB: 5LZK, 1.58 Å)

FAM83B DUF1669 domain (a.a 117-294) was buffered in 50 mM HEPES pH 7.5, 300 mM NaCl and concentrated to 12 mg/ml. Crystals were grown at 4°C in 150 nL sitting drops at a 1:1 protein: reservoir solution comprising 30.45% PEG3350, 0.2 M sodium iodide, 0.1 M bis-tris-propane pH 9.1 and 10% ethylene glycol. Before mounting, crystals were cryoprotected with mother liquor supplemented with an additional 25 % ethylene glycol and vitrified in liquid nitrogen. Diffraction data were collected at Diamond Light Source beamline I04. Diffraction data were processed using XDS (16) and molecular replacement was performed using PHASER (20) using 4URJ as the starting model. Model building and refinement were done using COOT (18) and PHENIX (19).

FAM83B Fragment screening (PDBs: [5HQI](#), [5HQJ](#), [5HQK](#), [5HQL](#), [5HQM](#), [5HQN](#), [5HQO](#), [5HQP](#), [5HQQ](#), [5HQR](#))

P2₁ crystal form: FAM83B DUF1669 domain (a.a 117-294) was buffered in 50 mM HEPES pH 7.5, 300 mM NaCl and concentrated to 13.1 mg/mL. Crystals were grown at 4°C in 300 nL sitting drops at a 1:2 protein: reservoir solution comprising 29% PEG3350, 0.1 M bis-tris-propane pH 8, 0.2 M NaI and 10% ethylene glycol. Fragments belonging to the DSPL1 library (500 mM in DMSO) were soaked at 20% fragment to drop volume for approximately 1 hour prior to addition of 20% ethylene glycol. Crystals were fished and vitrified in liquid nitrogen. Diffraction data were collected at Diamond Light Source beamline I04-1. Data was processed using either Xia2 (21) or autoPROC (22). Data was phased using DIMPLE (CCP4 suite (23)) and bound fragments identified using PanDDA (13) in the context of the XChemExplorer software suite. Bound fragments were refined using REFMAC (14).

P4₁22 crystal form: FAM83B DUF1669 domain (a.a 117-294) was buffered in 50 mM HEPES pH 7.5, 300 mM NaCl and concentrated to 12 mg/mL. Crystals were grown at 20°C in 600 nL sitting drops at a 2:3 protein: reservoir solution comprising 0.15 M NaCl and from 28.7-31.6% tacsimate. Fragments belonging to the DSPL2 and OxXchem libraries (500 mM in DMSO) were soaked at 20% fragment to drop volume for approximately 1 hour prior to addition of 20% ethylene glycol. Crystals were fished and vitrified in liquid nitrogen. Diffraction data were collected at Diamond Light Source beamline I04-1. Data was processed using either Xia2 (21) or autoPROC (22). Data was phased using DIMPLE (CCP4 suite (23)) and bound fragments identified using PanDDA (13) in the context of the XChemExplorer software suite. Bound fragments were refined using REFMAC (14).

FAM83B follow up fragment screening and structure determination (PDB: [5HQS](#), 1.95 Å)

FAM83B DUF1669 domain (a.a 117-294) was buffered in 50 mM HEPES pH 7.5, 300 mM NaCl and concentrated to 12 mg/mL. Crystals were grown at 20°C in 600 nL sitting drops at a 2:3 protein: reservoir solution comprising 0.15 M NaCl and from 28.7-31.6% tacsimate. Fragment follow-up compounds (200 mM in DMSO) were combined with mother liquor and ethylene glycol in a ratio of 1:7:2 and soaked for approximately 1 hour. Diffraction data were collected at Diamond Light Source beamline I04-1. Data was processed using either Xia2 (21) or autoPROC (22). Data was phased using DIMPLE (CCP4 suite (23)) and bound fragments identified using PanDDA (13) in the context of the XChemExplorer software suite. Bound fragments were refined using REFMAC (14).

Assays

Evaluation of fragment binding to FAM83B by SPR

SPR experiments were performed in 25 mM HEPES pH 7.5, 150 mM NaCl, 0.05% Tween-20, 2% DMSO. Biotinylated FAM83B and FAM83A were immobilized to approximately 6000 RU on streptavidin SPR chips (GE Healthcare) using a Biacore S200 surface plasmon resonance analyser. Fragments with a maximum concentration of 1 mM diluted in running buffer were injected for 15 seconds at 30 µL/min and the responses were recorded. The responses at 10 seconds after injection were analysed. The effects of any potential mismatch between the DMSO in the running buffer and that used for fragment dilution was corrected for.

Evaluation of casein kinase binding to FAM83B by Biolayer Interferometry (BLI)

BLI experiments used a buffer comprising 25 mM HEPES pH 7.5, 100 mM NaCl, 0.05% Tween-20, 0.1% BSA. Biotinylated FAM83B was immobilized onto streptavidin Octet sensors until saturation was observed. The sensors were then washed and dipped into wells of casein kinases at various concentrations up to 25 µM and the BLI signal recorded using an Octet RED384 system.

In vitro pull down assay for FAM83A binding to CSNK1E.

For in vitro pull down assay, all proteins and Ni-sepharose were equilibrated in binding buffer (50 mM HEPES pH 7.5, 500 mM NaCl, 5% glycerol, 5 mM imidazole) prior to use. 300 µg 6xHis-FAM83A (a.a. 122-304) was immobilised onto 200 µl Ni-sepharose and washed before addition of 100 µg CSNK1E. The Ni-sepharose was

then washed with binding buffer and the flow through collected. Two 1 mL wash steps were performed using binding buffer before bound proteins were eluted with 1 mL binding buffer supplemented with 250 mM imidazole. Fractions were run on a SDS-PAGE gel alongside the original protein solutions for molecular weight reference.

Other cellular and in vivo assays

Other cellular and in vivo assays are published (11,12).

References

1. Bartel, C. A., Parameswaran, N., Cipriano, R., and Jackson, M. W. (2016) [FAM83 proteins: Fostering new interactions to drive oncogenic signaling and therapeutic resistance](#). *Oncotarget* **7**, 52597-52612
2. Cipriano, R., Miskimen, K. L., Bryson, B. L., Foy, C. R., Bartel, C. A., and Jackson, M. W. (2014) [Conserved oncogenic behavior of the FAM83 family regulates MAPK signaling in human cancer](#). *Mol Cancer Res* **12**, 1156-1165
3. Snijders, A. M., Lee, S. Y., Hang, B., Hao, W., Bissell, M. J., and Mao, J. H. (2017) [FAM83 family oncogenes are broadly involved in human cancers: an integrative multi-omics approach](#). *Mol Oncol* **11**, 167-179
4. Li, Y., Dong, X., Yin, Y., Su, Y., Xu, Q., Zhang, Y., Pang, X., Zhang, Y., and Chen, W. (2005) [BJ-TSA-9, a novel human tumor-specific gene, has potential as a biomarker of lung cancer](#). *Neoplasia* **7**, 1073-1080
5. Chen, S., Huang, J., Liu, Z., Liang, Q., Zhang, N., and Jin, Y. (2017) [FAM83A is amplified and promotes cancer stem cell-like traits and chemoresistance in pancreatic cancer](#). *Oncogenesis* **6**, e300
6. Lee, S. Y., Meier, R., Furuta, S., Lenburg, M. E., Kenny, P. A., Xu, R., and Bissell, M. J. (2012) [FAM83A confers EGFR-TKI resistance in breast cancer cells and in mice](#). *J Clin Invest* **122**, 3211-3220
7. Cipriano, R., Graham, J., Miskimen, K. L., Bryson, B. L., Bruntz, R. C., Scott, S. A., Brown, H. A., Stark, G. R., and Jackson, M. W. (2012) [FAM83B mediates EGFR- and RAS-driven oncogenic transformation](#). *J Clin Invest* **122**, 3197-3210
8. Cipriano, R., Bryson, B. L., Miskimen, K. L., Bartel, C. A., Hernandez-Sanchez, W., Bruntz, R. C., Scott, S. A., Lindsley, C. W., Brown, H. A., and Jackson, M. W. (2014) [Hyperactivation of EGFR and downstream effector phospholipase D1 by oncogenic FAM83B](#). *Oncogene* **33**, 3298-3306
9. Yamaura, T., Ezaki, J., Okabe, N., Takagi, H., Ozaki, Y., Inoue, T., Watanabe, Y., Fukuhara, M., Muto, S., Matsumura, Y., Hasegawa, T., Hoshino, M., Osugi, J., Shio, Y., Waguri, S., Tamura, H., Imai, J. I., Ito, E., Yanagisawa, Y., Honma, R., Watanabe, S., and Suzuki, H. (2018) [Family with sequence similarity 83, member B is a predictor of poor prognosis and a potential therapeutic target for lung adenocarcinoma expressing wild-type epidermal growth factor receptor](#). *Oncol Lett* **15**, 1549-1558
10. Stuckey, J. A., and Dixon, J. E. (1999) [Crystal structure of a phospholipase D family member](#). *Nat Struct Biol* **6**, 278-284
11. Fulcher, L. J., Bozatzi, P., Tachie-Menson, T., Wu, K. Z. L., Cummins, T. D., Bufton, J. C., Pinkas, D. M., Dunbar, K., Shrestha, S., Wood, N. T., Weidlich, S., Macartney, T. J., Varghese, J., Gourlay, R., Campbell, D. G., Dingwell, K. S., Smith, J. C., Bullock, A. N., and Sapkota, G. P. (2018) [The DUF1669 domain of FAM83 family proteins anchor casein kinase 1 isoforms](#). *Sci Signal* **11**, eaao2341
12. Bozatzi, P., Dingwell, K. S., Wu, K. Z., Cooper, F., Cummins, T. D., Hutchinson, L. D., Vogt, J., Wood, N. T., Macartney, T. J., Varghese, J., Gourlay, R., Campbell, D. G., Smith, J. C., and Sapkota, G. P. (2018) [PAWS1 controls Wnt signalling through association with casein kinase 1alpha](#). *EMBO Rep* **19**
13. Pearce, N. M., Krojer, T., Bradley, A. R., Collins, P., Nowak, R. P., Talon, R., Marsden, B. D., Kelm, S., Shi, J., Deane, C. M., and von Delft, F. (2017) [A multi-crystal method for extracting obscured crystallographic states from conventionally uninterpretable electron density](#). *Nat Commun* **8**, 15123
14. Murshudov, G. N., Skubak, P., Lebedev, A. A., Pannu, N. S., Steiner, R. A., Nicholls, R. A., Winn, M. D., Long, F., and Vagin, A. A. (2011) [REFMAC5 for the refinement of macromolecular crystal structures](#). *Acta Crystallogr D Biol Crystallogr* **67**, 355-367

15. Knippschild, U., Kruger, M., Richter, J., Xu, P., Garcia-Reyes, B., Peifer, C., Halekotte, J., Bakulev, V., and Bischof, J. (2014) [The CK1 Family: Contribution to Cellular Stress Response and Its Role in Carcinogenesis](#). *Front Oncol* **4**, 96
16. Kabsch, W. (2010) [Xds](#). *Acta Crystallogr D Biol Crystallogr* **66**, 125-132
17. Terwilliger, T. C., Dimaio, F., Read, R. J., Baker, D., Bunkoczi, G., Adams, P. D., Grosse-Kunstleve, R. W., Afonine, P. V., and Echols, N. (2012) [phenix.mr_rosetta: molecular replacement and model rebuilding with Phenix and Rosetta](#). *J Struct Funct Genomics* **13**, 81-90
18. Emsley, P., and Cowtan, K. (2004) [Coot: model-building tools for molecular graphics](#). *Acta Crystallogr D Biol Crystallogr* **60**, 2126-2132
19. Adams, P. D., Afonine, P. V., Bunkoczi, G., Chen, V. B., Davis, I. W., Echols, N., Headd, J. J., Hung, L. W., Kapral, G. J., Grosse-Kunstleve, R. W., McCoy, A. J., Moriarty, N. W., Oeffner, R., Read, R. J., Richardson, D. C., Richardson, J. S., Terwilliger, T. C., and Zwart, P. H. (2010) [PHENIX: a comprehensive Python-based system for macromolecular structure solution](#). *Acta Crystallogr D Biol Crystallogr* **66**, 213-221
20. McCoy, A. J., Grosse-Kunstleve, R. W., Adams, P. D., Winn, M. D., Storoni, L. C., and Read, R. J. (2007) [Phaser crystallographic software](#). *J Appl Crystallogr* **40**, 658-674
21. Winter, G., Lobley, C. M., and Prince, S. M. (2013) [Decision making in xia2](#). *Acta Crystallogr D Biol Crystallogr* **69**, 1260-1273
22. Vonrhein, C., Flensburg, C., Keller, P., Sharff, A., Smart, O., Paciorek, W., Womack, T., and Bricogne, G. (2011) [Data processing and analysis with the autoPROC toolbox](#). *Acta Crystallogr D Biol Crystallogr* **67**, 293-302
23. Winn, M. D., Ballard, C. C., Cowtan, K. D., Dodson, E. J., Emsley, P., Evans, P. R., Keegan, R. M., Krissinel, E. B., Leslie, A. G., McCoy, A., McNicholas, S. J., Murshudov, G. N., Pannu, N. S., Potterton, E. A., Powell, H. R., Read, R. J., Vagin, A., and Wilson, K. S. (2011) [Overview of the CCP4 suite and current developments](#). *Acta Crystallogr D Biol Crystallogr* **67**, 235-242

TEP IMPACT

Publications arising from this work:

Fulcher LJ, Bozatz P, Tachie-Menson T, Wu KZL, Cummins TD, Bufton JC, Pinkas DM, Dunbar K, Shrestha S, Wood NT, Weidlich S, Macartney TJ, Varghese J, Gourlay R, Campbell DG, Dingwell KS, Smith JC, Bullock AN, Sapkota GP. (2018). [The DUF1669 domain of FAM83 family proteins anchor casein kinase 1 isoforms](#). *Sci Signal*. 11(531) eaao2341.

Grants arising from this work:

Grant: MRC Confidence in Concept Award

Project Title: Structure-guided design of FAM83B inhibitors for triple negative breast cancer

Amount awarded: £15,000

PI: Alex B Bullock (SGC Oxford)

Start date: 1 January 2018

End date: 30 September 2018

We respectfully request that this document is cited using the DOI value as given above if the content is used in your work.